Arabian Journal for Science and Engineering (2023) 48:3403–3423
https://doi.org/10.1007/s13369-022-07117-5

RESEARCH ARTICLE-MECHANICAL ENGINEERING

Multi-objective Optimization of Parameters in CNC Turning of a Hardened Alloy Steel Roll by Using Response Surface Methodology

Kashif Noor[1] · **Mubashir Ali Siddiqui**[1] · **Syed Amir Iqbal**[1]

Received: 31 October 2021 / Accepted: 28 June 2022 / Published online: 12 August 2022

Abstract
This study was conducted to optimize the machining parameters of the CNC turning operation of a large-sized, hardened alloy steel roll, at low cutting speed, and under wet machining conditions, which consumed minimum power and minimum specific energy to produce the machined surface with minimum surface roughness. A mixed-level statistical design was developed with four factors including cutting speed, feed, depth of cut, and tool insert type. Response surface methodology was used for the analysis and optimization of experimental results. The full quadratic response model and the main effect plots reported that the cutting speed was the most dominant factor for power consumption and feed for the specific energy consumption, while the most contributing factor for the surface roughness was feed. Cutting tool insert type was also found to be a significant factor. The effectiveness of the CBN and ceramic cutting tool was also compared by using contour plots. Desirability analysis showed that the optimized machining parameters were cutting speed of 41.23 m/min, feed of 0.1333 mm/rev, and depth of cut of 0.49 mm with CBN tool insert. This work compared the effectiveness of CBN and ceramic cutting tool inserts, at low cutting speeds under a wet machining environment. This work has also developed mathematical models for power consumption, specific energy consumption, and surface roughness. This research work also contributes to the practical industrial application of CNC turning in hot rolling mills.

Keywords CNC turning · Optimization · Power consumption · Energy consumption · Design of experiments · Response surface methodology

Abbreviations

V_c	Cutting speed
f	Feed
d	Depth of cut
L_W	Length of workpiece
D_w	Diameter of workpiece
E_s	Specific energy consumption
P	Power consumption in the machining stage
R_a	Surface roughness of a machined surface
Δ_i	Individual desirability for ith response
D	Composite desirability
y_i	iTh response
m	No. of responses
T	Target value
U	Upper bound
r	Desirability function index
$\overline{x}$	Mean value
DOE	Design of experiments
e-CDF	Empirical commutative distribution
S	Standard deviation
SS	The sum of squares
DF	Degree of freedom
MS	Mean squares
RSM	Response surface methodology
DOE	Design of experiments
e-CDF	Empirical commutative distribution
MRR	Material removal rate

✉ Kashif Noor
kashifnoor@neduet.edu.pk

[1] Department of Mechanical Engineering, NED University of Engineering and Technology, Karachi, Pakistan

1 Introduction

Turning of hard to machine materials like hardened steels or high alloy steels is always a challenge in the manufacturing industry due to excessive energy consumption in material removing of hardened materials. The high strength and wear-resistant properties of these hard alloy steel make them suitable for the manufacturing of machine tools, precision components used in automobiles, aircraft and rolling mills molding, and marine industries. In the analysis of energy consumption, a key dominant metric is power consumption, which consists of the machine power consumed by a machine tool's actions plus the cutting power needed to remove the desired material from the workpiece [1]. It closely relates to the specific energy consumption (SEC), i.e., the energy consumption for removing a unit volume of material from the workpiece [2]. For this reason, significant research has been done to develop predictive models for power consumption in machining. These models provide numerical relationships that enable manufacturers to optimize energy consumption and improve the energy efficiency of various material types.

Energy consumed in the hard turning process depends on the workpiece material, type of machine tool, machining parameters, cutting tool insert material and its geometrical features, tool path trajectory, and ultimately the wet or dry environmental conditions under which machining is performed.

In past, researchers have done extensive efforts to search for optimal machining parameters to minimize power consumption, minimum specific energy consumption, and to minimize the surface roughness, in the machining of different types of hardened steel, which is summarized in Table 1. Padhan et al., investigation of the power consumption of hardened AISI D3 steel by using nano-cutting fluid (graphene nanoparticle) revealed that energy consumption decreases under wet cutting conditions due to its efficient cooling and lubrication properties [3]. Benlahmidi et al. optimized the cutting parameters for minimum power consumption in turning hardened AISI H11 steel (50 HRC) with CBN tool inserts [4]. Chudy and Grzesik found that the power component consumed in material removal from hardened 41Cr4 (AISI 5140) steel was 20% of total power consumption in turning operation [5]. However, Żak used different shaped CBN insert tools to reveal that the actual power consumed in the hard turning operation of 41Cr4 alloy steel hardness was only 14% of the total power consumed [6]. The effect of machining parameters to optimize the energy efficiency, power factor, and active energy consumed by the machine in the machining of EN 353 alloy steel were investigated by Bilga et al. It reported that at optimum machining conditions, the power factor and energy efficiency were at the same level [7]. The power consumption of AISI D3 steel was optimized by Zerti et al. under a dry cutting environment [8]. Grzesik et al. investigated the effect of CBN tool nose radius on cutting power and specific cutting energy of hardened 41Cr4 alloy steel [9]. Park and Nguyen reduced the specific cutting energy to improve the energy efficiency of the hardened 4140 steel bar [10]. Nguyen et al. and Nguyen optimized the energy efficiency of hardened steel of 45 HRC and 51 HRC by using a self-propelled rotary tool [11, 12].

CBN and ceramic tool inserts are widely used in the manufacturing industry for the machining of various hard materials such as alloy steels, die steels, high-speed steels, bearing steels, white cast iron, and graphite cast iron. Various studies have been conducted to investigate the performance of CBN and ceramic tool inserts in the machining of various hard materials. For example, Benlahmidi et al. [4], Chudy and Grzesik [5], Żak [6], Grzesik, et al. [9], and Park and Nguyen [10] used CBN tool inserts to identify various factors affecting power and energy consumption in hard turning of various grades of hardened steels, whereas Zębala and Siwiec [13], Bouacha et al. [14], and Das et al. [15] identified various factors affecting cutting forces, surface roughness, and tool wear by conducting experiments in the turning operation of various grades of hardened steels by using CBN tools**.**

Ceramic tool insert was used by Zerti et al. [8] in the power consumption analysis of AISI D3 steel, while Bensouilah et al. [16], Suresh and Basavarajappa [17], and Davoudinejad and Noordin [18] used ceramic tool inserts to identified various factors affecting cutting forces, surface roughness, tool wear, tool life, and surface integrity by conducting experiments in turning operation of various grades of hardened steels. Benga and Abrao [19] used CBN and ceramic tool inserts to investigate the tool life and surface roughness on bearing steel. Aouici et al. [20] compared the performance of coated and uncoated ceramic tool wear on AISI H11 steel. Anthony [21] compared the effectiveness of ceramic tool insert type along with, cermet and coated carbide tool inserts to investigate the effect on the cutting force and chip morphology of AISI D2 steel.

This literature review identified that the majority of research work performed on hard turning was carried out under a dry machining environment at high cutting speeds. The comparison of the effectiveness of CBN and Ceramic tool insert under wet machining conditions was left unaddressed by the researchers. The CNC turning operations, on hardened steels, that are large in dimensions and that carry large weight, required a CNC turning operation at low cutting speeds.

The objective of this study was to find out the optimal machining parameters of CNC turning operation for hardened alloy steel roll that consumed the minimal power, and minimum specific energy to produce the machined surface of the roll, with minimum surface roughness, at a low cutting speed, and under wet machining conditions. This study also contributes to comparing the effectiveness of CBN and

Table 1 Literature overview of various studies in minimization of power consumption, energy consumption and surface roughness for tuning operation of hardened steel

Author	Workpiece material (hardness)	Cutting tool insert Type	Variable input factors	Env	Cutting speed levels	Work piece dimensions (mm)	Key findings
Padhan et al. [3]	AISI D3 steel	Uncoated carbides	Cutting speed, feed, depth of cut, tool nose radius	Wet	55 m/min, 95 m/min, 135 m/min	$D_w = 45$ mm, $L_w = 200$ mm	Optimized machining conditions reduced the energy consumption by 52.15%
Benlahmidi et al. [4]	AISI H11 steel (40–50 HRC)	CBN	Cutting speed, feed rate, depth of cut, workpiece hardness	Dry	120 m/min, 180 m/min, 240 m/min	Not mentioned	Surface roughness decreased with an increase in cutting speed, decrease in feed rate, increase in workpiece hardness, whereas depth of cut had a negligible effect
Chudy and Grzesik [5]	AISI 5140 steel (55 ± 1 HRC)	CBN	Cutting speed, feed rate, depth of cut	Wet	150 m/min, 200 m/min, 250 m/min and 300 m/min	Not mentioned	The energy-efficient process was performed at the maximum feed
Żak [6]	41Cr4 alloy steel (55 ± 1 HRC)	CBN	Tool corner radius		210 m/min (Constant)	Not mentioned	An increase in tool corner radius increases the surface roughness and increases the specific energy consumption
Bilga et al. [7]	EN 353 alloy steel	Tungsten carbide	Cutting speed, feed rate, depth of cut, tool nose radius	Wet	165.7 m/min, 207.2 m/min, and 248.6 m/min	$D_w = 44$ mm, $L_w = 98$ mm	Depth of cut is the most dominant parameter for power factor and energy efficiency
Zerti et al. [8]	AISI D3	Ceramic	Cutting speed, depth of cut, feed rate	Dry	220 m/min, 307 m/min, 440 m/min	$D_w = 70$ mm, $L_w = 400$ mm	Feed rate and cutting insert nose radius were the main influencing factors on surface roughness
Grzesik et al. [9]	41Cr4 alloy steel (55 ± 1 HRC)	CBN	Cutting speed, tool corner radius	Dry	150 m/min, 210 m/min and 270 m/min	Not mentioned	Tool corner radius influenced the surface roughness and tribological characteristics in hard machining

Table 1 (continued)

Author	Workpiece material (hardness)	Cutting tool insert Type	Variable input factors	Env	Cutting speed levels	Work piece dimensions (mm)	Key findings
Park and Nguyen [10]	4140 steel	CBN	Cutting speed, feed rate, tool nose radius, edge radius, rake angle	Dry	60 m/min, 180 m/min, 300 m/min	$D_w = 100$ mm, $L_w = 400$ mm	Optimized machining conditions reduced the specific energy by 14% and increased energy efficiency by 18%
Nguyen et al. [11]	Hardened steel (45 HRC)	Coated carbide	Cutting speed, feed rate, depth of cut, inclined angle	Dry	100 m/min, 150 m/min, 200 m/min	$D_w = 40$ mm, $L_w = 260$ mm	The highest values of the depth of cut, cutting speed, and feed rate can be used to enhance energy efficiency. The lowest values of the depth of cut and feed rate were recommended to decrease the roughness
Nguyen [12]	Hardened steel (51 HRC)	Coated carbide	Cutting speed, feed rate, depth of cut, inclined angle	Dry	100 m/min, 150 m/min, 200 m/min	$D_w = 40$ mm, $L_w = 280$ mm	Feed, speed, depth of cut, and inclined angle were the affecting factors for specific energy. The low values of the depth of cut and feed rate decreased the roughness
Zębala and Siwiec [13]	Cold work tool steel (56.5–62 HRC)	CBN	Cutting speed, feed rate, depth of cut, workpiece hardness	Dry	120 m/min (constant)	$D_w = 90$ mm, (Length was not mentioned)	The higher hardness of the workpiece material reduced surface roughness. The cutting speed and depth of cut had a smaller influence on the surface roughness than the feed rate
Bouacha et al. [14]	AISI 52,100 bearing steel (64 HRC)	CBN	Cutting speed, feed rate, depth of cut	Dry	125 m/min, 126 m/min, 246 m/min	$D_w = 56$ mm, $L_w = 400$ mm	The surface roughness was highly affected by feed rate, whereas the cutting speed had a negative effect and the depth of cut has negligible influence

Table 1 (continued)

Author	Workpiece material (hardness)	Cutting tool insert Type	Variable input factors	Env	Cutting speed levels	Work piece dimensions (mm)	Key findings
Das et al. [15]	AISI 52,100 steel	CBN	Cutting speed, feed, depth of cut	Dry	100 m/min, 140 m/min, 200 m/min	$D_w = 41$ mm, $L_w = 300$ mm	The feed and cutting speed strongly influenced the surface roughness
Bensouilah et al. [16]	AISI D3 steel (63 HRC)	Coated and uncoated Ceramic	Cutting speed, feed rate, depth of cut, cutting tool insert material	Dry	75 m/min, 105 m/min, 150 m/min, 210 m/min	Not mentioned	The coated ceramic insert had a better performance on surface roughness as compared with the uncoated ceramic insert
Suresh and Basavarajappa [17]	AISI H13 Steel (55 HRC)	Coated Ceramic	Cutting speed, feed rate, depth of cut	Dry	42 m/min, 80 m/min, 140 m/min, 200 m/min, 238 m/min	$D_w = 100$ mm, $L_w = 400$ mm	The feed was the highest contributing factor for surface roughness, followed by cutting speed whereas depth of cut had minimum effect
Davoudinejad and Noordin [18]	DF-3 tool steel (58 HRC)	Coated Ceramic	Cutting speed, feed rate, tool edge geometry (Chamfered/Honed)	Dry	100 m/min, 150 m/min, 210 m/min	$D_w = 92$ mm, $L_w = 220$ mm	chamfered edge cutting tool produced lower surface roughness as compared to a honed edge
Benga and Abrao [19]	100Cr6 bearing steel (62–64 HRC)	Ceramic, CBN	Cutting speed, feed rate, cutting tool insert material	Dry	100 m/min, 116 m/min, 132 m/min, 148 m/min, 164 m/min, 180 m/min	$D_w = 60$ mm, $L_w = 500$ mm (Tube)	At low cutting speeds, the heat generation required to reduce the work material shear strength was not enough and higher cutting forces were required, affecting the surface finish negatively. At high cutting speed, the possibility of chatters increased, damaging the surface finish

Table 2 Chemical analysis of alloy steel roll used in the experimental work

Elements	C	Si	Cr	V	W	Mo	Ni	Mn	Fe	Rest
Conc (%)	2.25	1.16	2.6	1.67	0.81	1.36	0.52	0.5	87.8	others

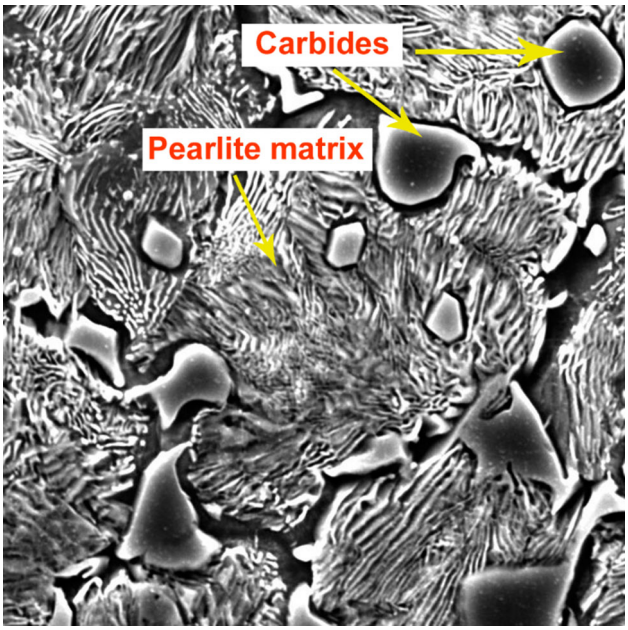

Fig. 1 SEM image of the hardened alloy steel roll showing its microstructure

ceramic cutting tool inserts under the wet machining environment of hardened alloy steel roll at low cutting speeds. The experimental work was performed on an actual large-diameter-sized, hardened steel roll of a hot rolling mill in the actual industrial environment with the industrial parameters that could incorporate the factors that can affect the results of this research. This makes it a distinguishable work among other researchers' work.

2 Material and Method

2.1 Material

The workpiece material used in this study for machining operation was hardened alloy steel roll, manufactured by Camet. The material specification of the alloy steel roll is shown in Table 2. The diameter of the hardened steel alloy roll was 315 mm. The overall length of the roll was 1426 mm, while the barrel portion of the roll was 700 mm in length. The barrel was that portion of the roll that was used for the CNC turning operation. The weight of the hardened alloy steel roll was 538 kg. Figure 1 illustrates the microstructure of the alloy steel roll material that was performed on the Tescan VEGA3 series at 1000X. The image shows that the alloy roll has a pearlite structure of matrix with primary and secondary carbides.

2.2 Method

The methodology was comprised of the design of experiments, selection of input factors for experimental setup, execution of CNC turning, and collection of response data as shown in Fig. 2

2.2.1 Design of Experiment

Statistical methods, especially in the domain of design of experiments (DOE), are a very useful tool for data analyses. In this study, a mixed-level design ($2^1 \times 3^3$) with four machining input factors including cutting speed, feed, depth of cut, and tool insert type was used for the experimental design. Tool insert was a categorical factor with two levels, while cutting speed, feed, and depth of cut were three-level continuous factors as shown in Table 3, thus resulting in fifty-four treatment combinations. These factors and associated levels were defined according to the machine capacity and Union materials cutting tool catalog. The recommended machining parameters for finish hard turning of steel (H $\geq$ 45 HRC) by the Union materials cutting tool catalog were, 40 m/min $\leq V_c \leq$ 200 m/min, 0.05 mm/rev $\leq f \leq$ 0.5 mm/rev, and 0.1 mm $\leq d \leq$ 0.5 mm. The low cutting speed levels were selected because of the high weight of the roll, i.e., 538 kg, and the large-sized dimensions of the hardened alloy steel roll, i.e., 1426 mm overall length of the roll. The analysis of results and the optimization were carried out on Minitab 19 software.

2.2.2 Experimental Setup

CNC lathe CK8470 × 3500 with SINUMERIK 828D-CNC system was used to perform the experimental runs. The machine size used was 7450 × 2280 × 1950. The spindle chuck had a diameter of 650 mm, and it could clamp the workpiece of diameter ranging from 85 to 500 mm. The main motor had a power capacity of 37 kW. The maximum limit of workpiece load and length that can mount was 6-ton and 3500 mm, respectively. The hardened alloy steel roll used for this experimental run was a large-sized workpiece. The roll diameter was 315 mm, the overall length of the roll was

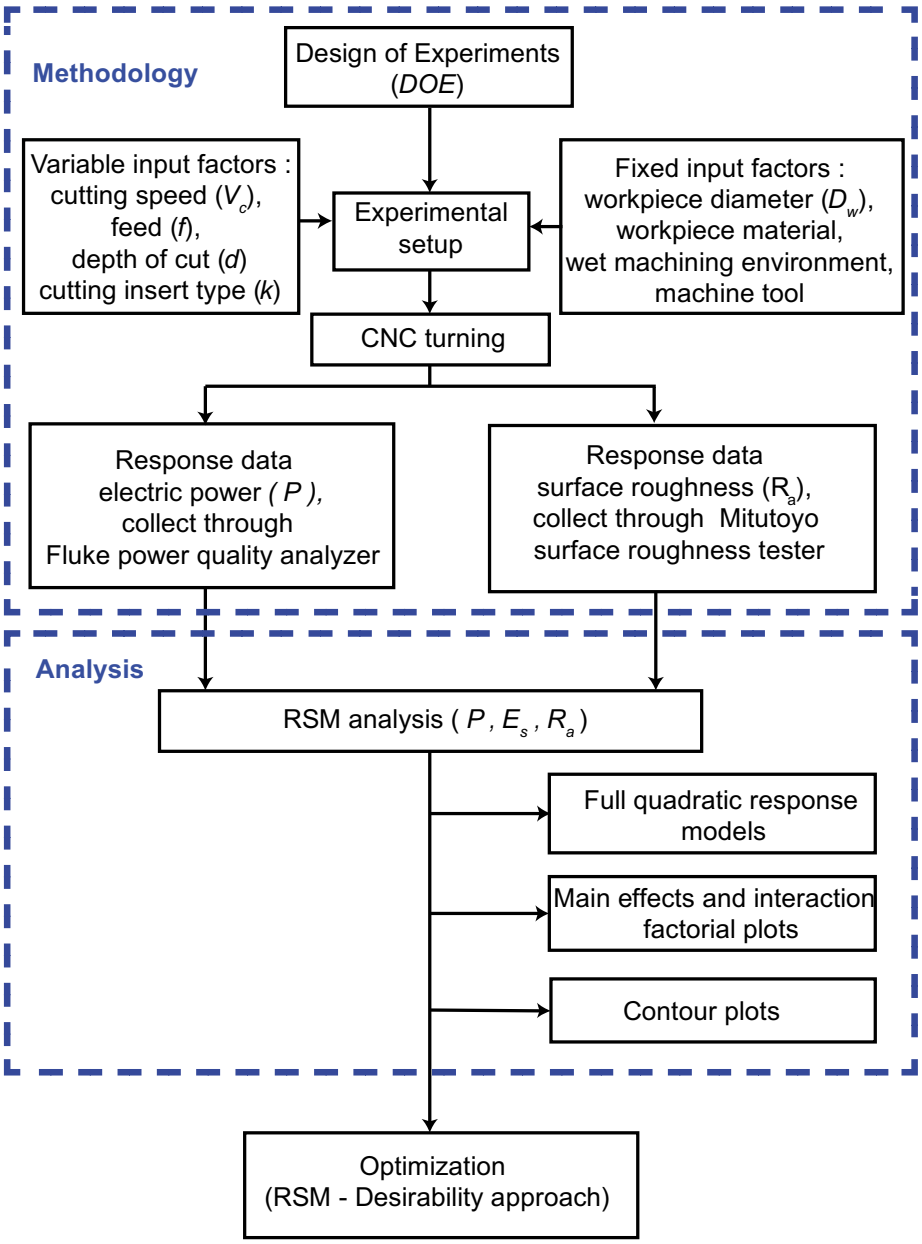

Fig. 2 Methodology showing the sequence of various work performed

Table 3 Input factors in the design of experiments, with their levels and design points

Symbol	Factors	Units	No. of Levels	Level 1	Level 2	Level 3
V_c	Cutting Speed	m/min	3	40	45	50
f	Feed	mm/rev	3	0.1	0.15	0.2
d	Depth of cut	mm	3	0.3	0.4	0.5
k	Cutting tool insert type	–	2	1*	2**	–

*CBN cutting tool insert, **Ceramic cutting tool insert

Table 4 Matrix for the design of experiments with responses

Set of experiments	Factors				Responses								
	V_c (m/min)	f (mm/rev)	d (mm)	k	P (kW)			E_s (kJ/mm^3)			R_a (μm)		
					1st Obs	2nd Obs	3rd Obs	1st Obs	2nd Obs	3rd Obs	1st Obs	2nd Obs	3rd Obs
1	40	0.10	0.3	1	2.38	2.39	2.47	1.52	1.53	1.60	0.548	0.547	0.547
2	40	0.10	0.4	1	2.5	2.52	2.48	1.22	1.23	1.20	0.543	0.541	0.542
3	40	0.10	0.5	1	2.56	2.57	2.55	1.00	1.01	1.00	0.603	0.602	0.601
4	40	0.15	0.3	1	2.62	2.65	2.61	1.15	1.16	1.14	0.751	0.753	0.752
5	40	0.15	0.4	1	2.67	2.78	2.61	0.88	0.93	0.86	0.745	0.747	0.746
6	40	0.15	0.5	1	2.71	2.84	2.71	0.72	0.76	0.72	0.831	0.830	0.820
7	40	0.20	0.3	1	2.68	2.67	2.57	0.89	0.88	0.84	1.553	1.551	1.552
8	40	0.20	0.4	1	2.79	2.68	2.74	0.70	0.66	0.68	1.553	1.552	1.551
9	40	0.20	0.5	1	2.79	2.84	2.72	0.56	0.57	0.54	1.554	1.552	1.553
10	45	0.10	0.3	1	2.83	2.79	2.85	1.68	1.65	1.70	0.497	0.496	0.497
11	45	0.10	0.4	1	2.79	2.86	2.85	1.24	1.28	1.27	0.493	0.494	0.494
12	45	0.10	0.5	1	2.82	2.98	2.98	1.01	1.08	1.08	0.494	0.496	0.495
13	45	0.15	0.3	1	2.86	3.11	2.96	1.14	1.26	1.19	0.686	0.687	0.688
14	45	0.15	0.4	1	3.03	3.05	3.02	0.92	0.92	0.91	0.686	0.684	0.686
15	45	0.15	0.5	1	3.04	3.07	3.02	0.74	0.74	0.73	0.760	0.758	0.758
16	45	0.20	0.3	1	2.99	3.12	3.02	0.90	0.95	0.91	1.330	1.332	1.331
17	45	0.20	0.4	1	3.01	3.1	3.02	0.68	0.71	0.68	1.324	1.323	1.323
18	45	0.20	0.5	1	3.11	3.07	3.04	0.57	0.56	0.55	1.370	1.360	1.370
19	50	0.10	0.3	1	2.92	2.97	2.97	1.58	1.61	1.61	0.394	0.393	0.393
20	50	0.10	0.4	1	2.92	2.99	2.99	1.18	1.22	1.22	0.390	0.391	0.389
21	50	0.10	0.5	1	3.05	3.1	3.06	1.00	1.02	1.00	0.397	0.398	0.397
22	50	0.15	0.3	1	3.02	3.11	3.06	1.10	1.14	1.11	0.632	0.634	0.633
23	50	0.15	0.4	1	3.09	3.13	3.09	0.84	0.86	0.84	0.630	0.631	0.629
24	50	0.15	0.5	1	3.12	3.2	3.16	0.68	0.71	0.69	0.686	0.698	0.698
25	50	0.20	0.3	1	3.08	3.11	3.14	0.84	0.85	0.86	1.444	1.442	1.443
26	50	0.20	0.4	1	3.61	3.68	3.66	0.76	0.78	0.78	1.438	1.432	1.436
27	50	0.20	0.5	1	3.73	3.97	3.91	0.63	0.68	0.67	1.459	1.458	1.459
28	40	0.10	0.3	2	2.9	2.89	2.9	1.95	1.95	1.95	0.589	0.587	0.587
29	40	0.10	0.4	2	2.93	2.92	2.99	1.48	1.48	1.52	0.586	0.585	0.584
30	40	0.10	0.5	2	2.97	2.91	2.92	1.21	1.18	1.18	0.603	0.598	0.598
31	40	0.15	0.3	2	2.98	2.99	2.85	1.35	1.35	1.27	0.995	0.997	0.986
32	40	0.15	0.4	2	2.95	2.96	2.99	1.00	1.00	1.01	0.991	0.992	0.981
33	40	0.15	0.5	2	3.01	3.03	3.02	0.82	0.82	0.82	1.366	1.361	1.360
34	40	0.20	0.3	2	2.97	3.03	3.05	1.01	1.03	1.04	2.325	2.200	2.300
35	40	0.20	0.4	2	3.03	3	3.05	0.77	0.76	0.78	1.950	1.980	1.960
36	40	0.20	0.5	2	3.03	3.07	3.03	0.62	0.63	0.62	2.113	2.116	2.117
37	45	0.10	0.3	2	3.02	3.06	3.08	1.83	1.85	1.87	0.576	0.588	0.587
38	45	0.10	0.4	2	3.1	3.05	3.05	1.41	1.39	1.39	0.532	0.534	0.533

Table 4 (continued)

Set of experiments	Factors				Responses								
	V_c (m/min)	f (mm/rev)	d (mm)	k	P (kW)			E_s (kJ/mm^3)			R_a (μm)		
					1st Obs	2nd Obs	3rd Obs	1st Obs	2nd Obs	3rd Obs	1st Obs	2nd Obs	3rd Obs
39	45	0.10	0.5	2	3.07	3.09	3.05	1.12	1.13	1.11	0.585	0.588	0.589
40	45	0.15	0.3	2	3.08	3.11	3.11	1.25	1.26	1.26	0.992	0.992	0.994
41	45	0.15	0.4	2	3.09	3.13	3.2	0.94	0.95	0.98	0.989	0.901	0.902
42	45	0.15	0.5	2	3.12	3.18	3.12	0.76	0.78	0.76	1.366	1.348	1.348
43	45	0.20	0.3	2	3.12	3.22	3.17	0.95	0.99	0.97	1.847	1.846	1.847
44	45	0.20	0.4	2	3.11	3.36	3.32	0.71	0.78	0.77	1.840	1.842	1.843
45	45	0.20	0.5	2	3.28	3.29	3.27	0.61	0.61	0.60	1.857	1.858	1.856
46	50	0.10	0.3	2	3.22	3.18	3.22	1.78	1.75	1.78	0.472	0.471	0.475
47	50	0.10	0.4	2	3.2	3.3	3.31	1.32	1.37	1.38	0.468	0.469	0.469
48	50	0.10	0.5	2	3.29	3.2	3.24	1.09	1.06	1.07	0.483	0.498	0.498
49	50	0.15	0.3	2	3.17	3.32	3.2	1.16	1.23	1.18	1.011	1.021	1.022
50	50	0.15	0.4	2	3.4	3.21	3.47	0.95	0.88	0.97	0.929	0.933	0.934
51	50	0.15	0.5	2	3.48	3.59	3.55	0.78	0.81	0.80	1.166	1.171	1.172
52	50	0.20	0.3	2	3.59	3.76	3.73	1.01	1.07	1.06	1.832	1.835	1.833
53	50	0.20	0.4	2	3.75	3.82	3.82	0.80	0.82	0.82	1.810	1.792	1.803
54	50	0.20	0.5	2	3.95	4.07	4.09	0.68	0.70	0.71	1.955	1.958	1.959

1426 mm, and it carried 538 kg weight, which was within the specified limits of the CNC lathe.

Diamond-shaped inserts of CBN and ceramic with identical dimensions were used to study the effect of tool insert material. The CBN tool insert had an ISO designation number DNGA 150608 R1, grade SBN1000 made by Union Materials Corporation. The ceramic tool insert had an ISO designation number DNGA 150608 E040, grade ST500 made by Union Materials Corporation. A tool holder having designation number TDJNR 2525 M15 was employed to hold these tool inserts. The experiment was performed under wet environmental machining conditions by using Byco Socol soluble cutting oil having a viscosity index of 116. The workpiece diameter was kept constant for all experimental trials. A new insert was employed before each experimental run as it has already been found that the average specific cutting energy increases, as tool wear increases [22, 23].

2.2.3 Response Data Collection

The response data were collected for the surface roughness generated on the workpiece and the power consumed by the CNC lathe in the machining stage of the hardened alloy steel roll. Mitutoyo surface roughness tester was used to record the surface roughness values, while Fluke 43B power quality analyzer was employed to capture the total power consumption during machining of hardened alloy steel roll. The experimental data were recorded online on a laptop for each set of experiments and analyzed with the aid of Fluke 43B software. A total of fifty-four treatment combinations with three replicates each were recorded, as listed in Table 4. A new tool insert was used for each experimental trial under a wet machining environment. The workpiece material, machine tool setup, and response recording setup are shown in Fig. 3.

3 Results and Discussion

The total power consumed by the CNC lathe machine in the machining stage is the summation of the cutting power and the idle power consumed by the machine as expressed in Eq. (1)

$$P = P_c + P_o, \tag{1}$$

where P is the total power consumed by the CNC lathe in the machining stage, P_o is the idle power and P_c is the cutting power. P_o corresponds to the power demand to turn on: the main motor for rotating the workpiece; feed motor for movement of the cutting tool; coolant system; hydraulic pump; and computer console. P_o can vary from one machine tool

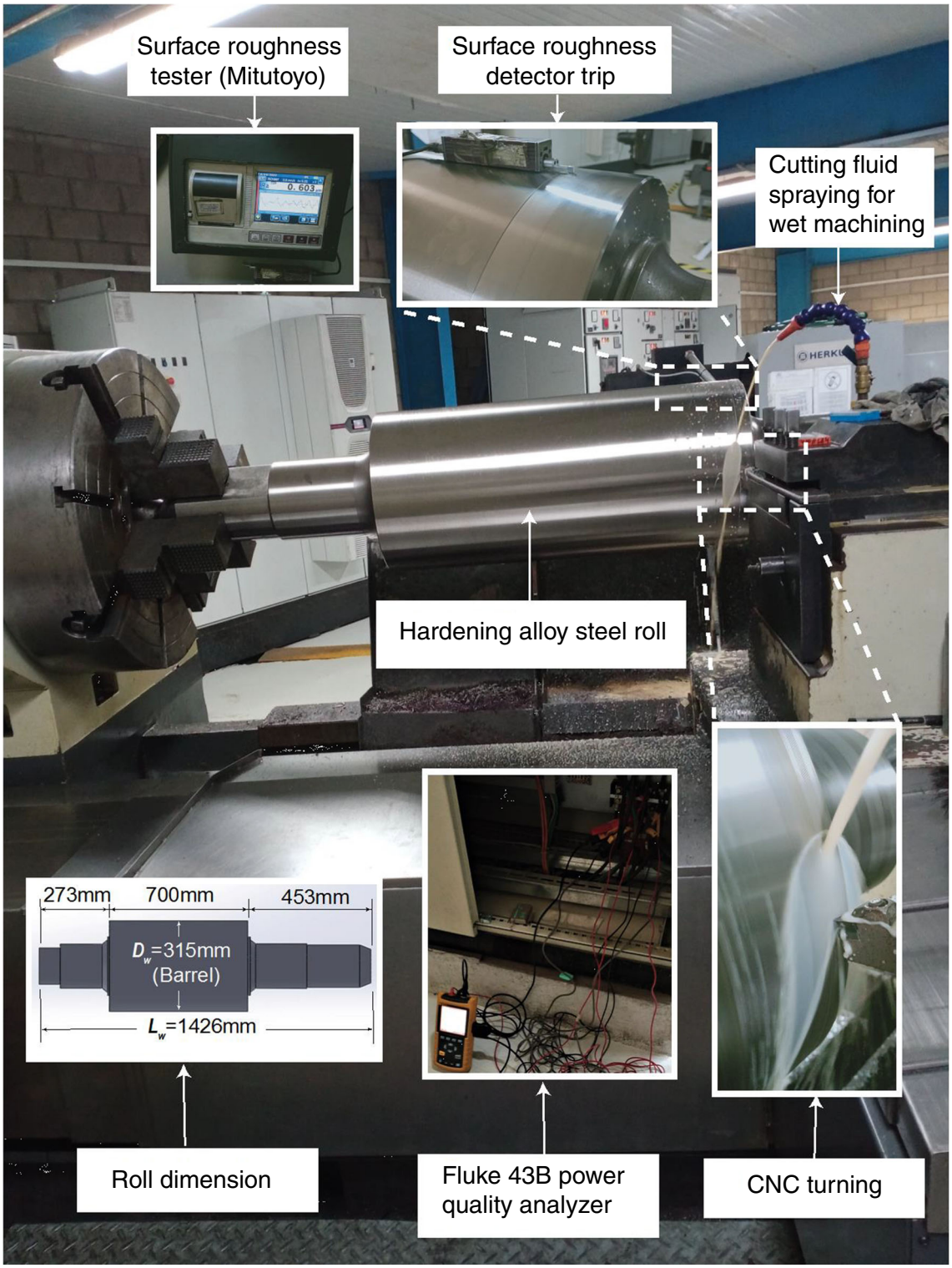

Fig. 3 Experimental setup for CNC turning, Fluke 4B analyzer setup, and the surface roughness tester used for the collection of response data

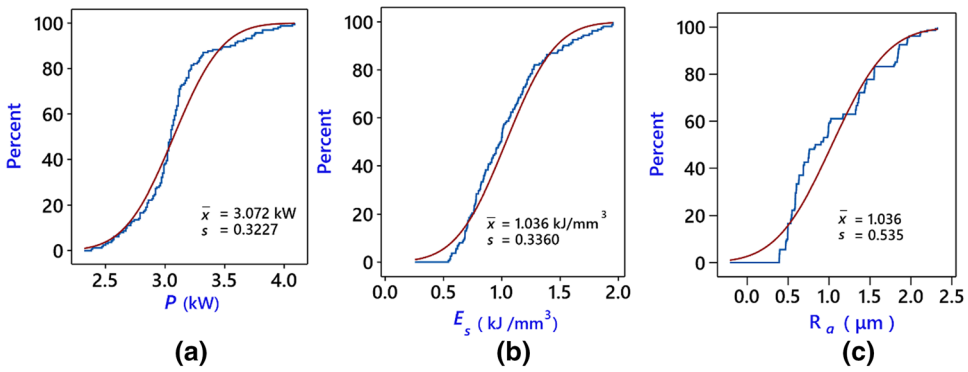

Fig. 4 Empirical CDF **a** power consumption, **b** specific energy consumption and **c** surface roughness

Table 5 Regression equations developed by RSM for power consumption, specific energy consumption, and surface roughness

Insert type (k)	Regression equations
CBN ($k = 1$)	$P = 6.00 - 0.1051\ V_c - 22.48\ f - 3.84\ d + 0.000726\ {V_c}^2 + 13.81\ f^2 - 0.77\ d^2 + 0.4083\ V_c \times f + 0.0919\ V_c \times d + 7.97\ f \times d$
Ceramic ($k = 2$)	$P = 6.76 - 0.1124\ V_c - 22.78\ f - 4.16\ d + 0.000726\ {V_c}^2 + 13.81\ f^2 - 0.77\ d^2 + 0.4083\ V_c \times f + 0.0919\ V_c \times d + 7.97\ f \times d$
CBN ($k = 1$)	$E_s = 6.440 - 0.0163\ V_c - 30.67\ f - 10.398\ d - 0.000115\ {V_c}^2 + 44.18\ f^2 + 5.747\ d^2 + 0.1173\ V_c \times f + 0.02567\ V_c \times d + 16.443\ f \times d$
Ceramic ($k = 2$)	$E_s = 7.197 - 0.0235\ V_c - 31.66\ f - 10.824\ d - 0.000115\ {V_c}^2 + 44.18\ f^2 + 5.747\ d^2 + 0.1173\ V_c \times f + 0.02567\ V_c \times d + 16.443\ f \times d$
CBN ($k = 1$)	$R_a = 5.66 - 0.1518\ V_c - 13.31\ f - 5.17\ d + 0.0001595\ {V_c}^2 + 82.98\ f^2 + 6.67\ d^2 - 0.0388\ V_c \times f + 0.0020\ V_c \times d - 0.55\ f \times d$
Ceramic ($k = 2$)	$R_a = 5.25 - 0.1532\ V_c - 8.59\ f - 4.85\ d + 0.0001595\ {V_c}^2 + 82.98\ f^2 + 6.67\ d^2 - 0.0388\ V_c \times f + 0.0020\ V_c \times d - 0.55\ f \times d$

Table 6 Full quadratic response surface design model for power consumption

Source	DF	Adj SS	Adj MS	F-value	p value	CR (%)	Remarks
Model	13	15.0499	1.15768	99.77	0.000	89.76	Significant
Linear	4	13.905	3.47625	299.57	0.000	82.93	Significant
V_c	1	8.0579	8.05787	694.4	0.000	48.06	Significant
f	1	2.5607	2.56071	220.67	0.000	15.27	Significant
d	1	0.559	0.55901	48.17	0.000	3.33	Significant
k	1	2.7274	2.72741	235.04	0.000	16.27	Significant
Square	3	0.0569	0.01897	1.64	0.184	0.34	Not Significant
V_c^2	1	0.0119	0.01186	1.02	0.314	0.07	Not Significant
f^2	1	0.0429	0.04294	3.7	0.056	0.26	Not Significant
d^2	1	0.0021	0.00213	0.18	0.669	0.01	Not Significant
2-Way interaction	6	1.088	0.18133	15.63	0.000	6.49	Significant
$V_c \times f$	1	0.7503	0.75031	64.66	0.000	4.47	Significant
$V_c \times d$	1	0.1522	0.15217	13.11	0.000	0.91	Significant
$V_c \times k$	1	0.0363	0.0363	3.13	0.079	0.22	Not Significant
$f \times d$	1	0.1144	0.1144	9.86	0.002	0.68	Significant
$f \times k$	1	0.0058	0.00578	0.5	0.481	0.03	Not Significant
$d \times k$	1	0.029	0.02901	2.5	0.116	0.17	Not Significant
Residual error	148	1.7174	0.0116				

Table 6 (continued)

Source	DF	Adj SS	Adj MS	F-value	p value	CR (%)	Remarks
Lack-of-fit	40	1.3641	0.0341	10.43	0.000		
Pure error	108	0.3533	0.00327				
Total	161	16.7673					

$S = 0.1077$; $R^2 = 89.76\%$; R^2 (adj.) $= 88.86\%$; R^2 (pred.) $= 87.60\%$

Table 7 Full quadratic response surface design for specific energy consumption

Source	DF	Adj SS	Adj MS	F-value	p value	CR (%)	Remarks
Model	13	17.9133	1.37794	769.81	0.000	98.54	Significant
Linear	4	16.6445	4.16113	2324.66	0.000	91.56	Significant
V_c	1	0.0147	0.01471	8.22	0.005	0.08	Significant
f	1	9.9083	9.90827	5535.38	0.000	54.51	Significant
d	1	6.1797	6.17974	3452.39	0.000	34.00	Significant
k	1	0.5418	0.54178	302.67	0.000	2.98	Significant
Square	3	0.5584	0.18615	103.99	0.000	3.07	Significant
V_c^2	1	0.0003	0.0003	0.17	0.685	0.00	Not Significant
f^2	1	0.4392	0.43924	245.39	0.000	2.42	Significant
d^2	1	0.1189	0.11891	66.43	0.000	0.65	Significant
2-way Interaction	6	0.7103	0.11839	66.14	0.000	3.91	Significant
$V_c \times f$	1	0.0619	0.06193	34.6	0.000	0.34	Significant
$V_c \times d$	1	0.0119	0.01186	6.62	0.011	0.07	Not Significant
$V_c \times k$	1	0.0347	0.03472	19.4	0.000	0.19	Significant
$f \times d$	1	0.4867	0.48665	271.87	0.000	2.68	Significant
$f \times k$	1	0.0662	0.06619	36.98	0.000	0.36	Significant
$d \times k$	1	0.049	0.04897	27.36	0.000	0.27	Significant
Residual Error	148	0.2649	0.00179				
Lack-of-fit	40	0.21	0.00525	10.33	0.00		
Pure Error	108	0.0549	0.00051				
Total	161	18.1782					

$S = 0.042$ $R^2 = 98.54\%$ R^2 (adj.) $= 98.41\%$ R^2 (pred.) $= 98.24\%$

to another. P_c is the actual power consumed in removing the material from the workpiece during machining, P_c can be expressed as the summation of the power spent on the plastic deformation of the layer being removed and power lost in friction at the tool-chip interface and tool-workpiece. It is expressed in Eq. (2)

$$P_c = P_s + P_f \tag{2}$$

where P_s and P_f denote the shear power and friction power. Here, it is obvious that the workpiece and the cutting tool with its subordinate insert influence P_c.

Specific cutting energy (E_s) in machining is the energy required to remove a unit volume of material from the workpiece as given by Eq. (3)

$$E_s = \frac{P_c}{\text{MRR}} = \frac{P - P_o}{f \times d \times V_c}, \tag{3}$$

where MRR, f, d, and V_c denote the material removal rate, feed, depth of cut, and cutting speed, respectively.

Statistical data revealed that the minimum and maximum values for power consumption were 2.38 kW and 4.09 kW, for specific energy consumption was found to be 0.54 kJ/mm^3 and 1.95 kJ/mm^3, and for surface roughness was found to be 0.38 μm to 2.211 μm, respectively. Empirical cumulative

Table 8 Full quadratic response surface design for surface roughness of hard alloy steel roll

Source	DF	Adj SS	Adj MS	F-value	p value	CR (%)	Remarks
Model	13	45.2061	3.4774	514.94	0.000	97.84	Significant
Linear	4	42.1204	10.5301	1559.33	0.000	91.16	Significant
V_c	1	0.5298	0.5298	78.45	0.000	1.15	Significant
f	1	37.5889	37.5889	5566.3	0.000	81.35	Significant
d	1	0.1221	0.1221	18.08	0.000	0.26	Significant
k	1	3.8797	3.8797	574.51	0.000	8.40	Significant
Square	3	1.7669	0.589	87.21	0.000	3.82	Significant
V_c^2	1	0.0572	0.0572	8.47	0.004	0.12	Significant
f^2	1	1.5493	1.5493	229.43	0.000	3.35	Significant
d^2	1	0.1603	0.1603	23.74	0.000	0.35	Significant
2-Way interaction	6	1.3188	0.2198	32.55	0.000	2.85	Significant
$V_c \times f$	1	0.0068	0.0068	1	0.318	0.01	Not Significant
$V_c \times d$	1	0.0001	0.0001	0.01	0.918	0.00	Not Significant
$V_c \times k$	1	0.0013	0.0013	0.19	0.664	0.00	Not Significant
$f \times d$	1	0.0005	0.0005	0.08	0.777	0.00	Not Significant
$f \times k$	1	1.2825	1.2825	189.92	0.000	2.78	Significant
$d \times k$	1	0.0277	0.0277	4.1	0.045	0.06	Significant
Residual Error	148	0.9994	0.0068				
Lack-of-fit	40	0.9839	0.0246	170.51	0.000		
Pure Error	108	0.0156	0.0001				
Total	161	46.2055					

$S = 0.082$; $R^2 = 97.84\%$; R^2 (adj.) $= 97.65\%$; R^2 (pred.) $= 97.41\%$

distribution function (e-CDF) for power consumption, specific energy consumption, and surface roughness are shown in Fig. 4a–c, respectively, confirming a close fit by the normal curve. The mean value for power consumption, specific energy consumption, and surface roughness was found to be 3.072 kW, 1.03 kJ/mm^3, and 1.027 μm, respectively.

3.1 Analysis and Optimization by Response Surface Methodology

Process parameters optimization was performed by using the response surface methodology (RSM) tool. RSM is a dominating methodology to analyze the outcomes of experiments for optimum response. It is a statistical technique that comprises design matrices having input variables and output variable(s). These input variables potentially influence the output variable(s). It is not only considered a tool, to search for the optimum solution, but it is also used to build empirical models among input and output variables. The input variables (cutting speed, feed, depth of cut, and tool insert) were independent variables, while the output variables (power consumption, specific energy consumption, and surface roughness) were the dependent variables in the design matrix of RSM. The mathematical function developed by RSM depends on the system's response. If responses of the system fit well as a linear function of input factors, it reveals that the empirical model is based on a first-order polynomial equation. However, if there is a curve on the response surface of the RSM model, higher-order polynomial equations should be used for estimating the response model. Another important feature of the RSM is its desirability function. A desirability function is an effective tool for exploring the optimum condition(s) for the desired response target.

3.1.1 Full Quadratic Response Surface Design

Experimental investigations have found that in the machining operation, empirical models of first-order, second-order, and exponential models were fit for power and energy consumption [24, 25]. For this study, a full quadratic model was selected. The significance of adding quadratic terms to the two factor's interaction was tested by p value. A full quadratic analysis of variance with a 95% confidence level for power consumption, specific energy consumption, and surface roughness was developed. The values of R^2 were 89.76%, R^2 (adj.) was 88.86% and R^2 (Pred.) was 87.6%

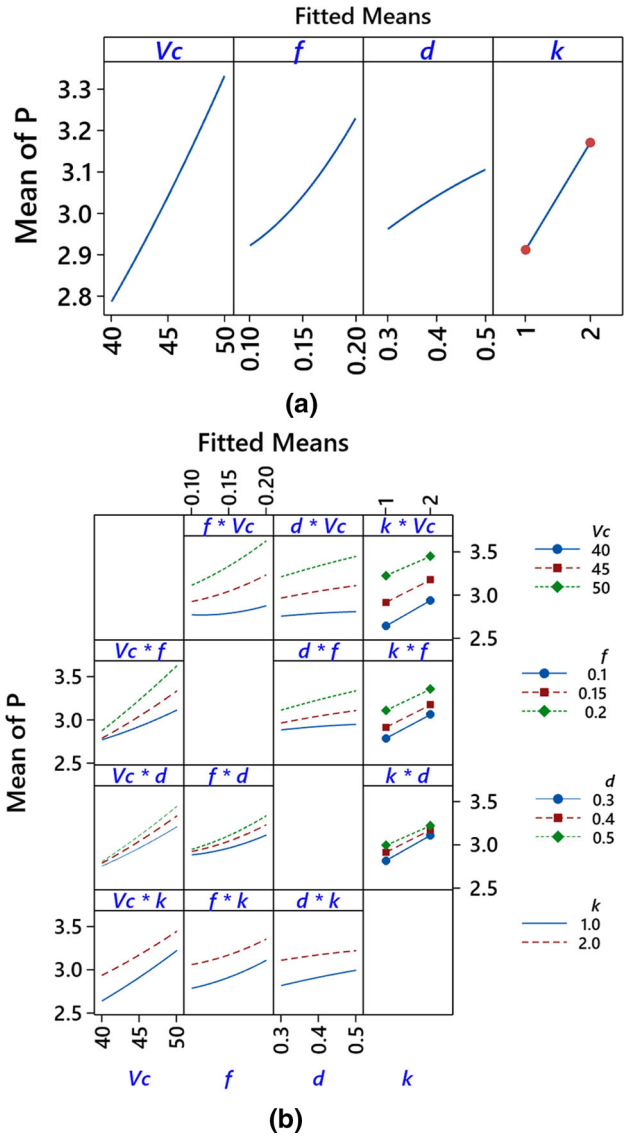

Fig. 5 Factorial plots for power consumption in the machining stage of the hardened alloy steel roll. **a** Main effect plots, **b** two-way factorial interaction

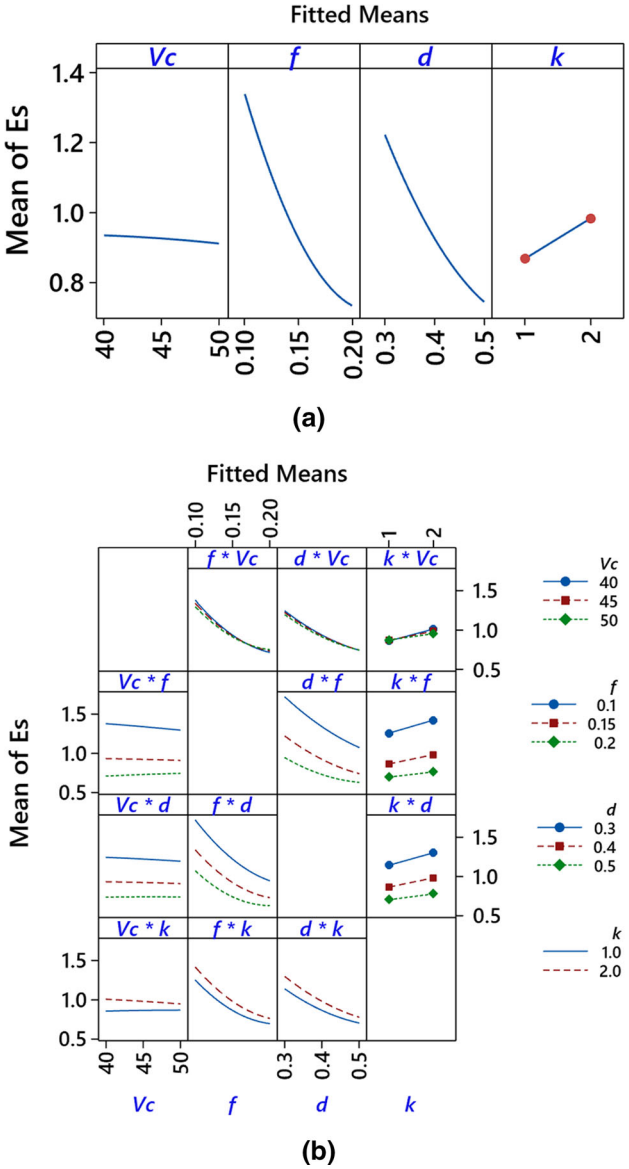

Fig. 6 Factorial plots for specific energy consumption in the machining stage of the hardened alloy steel roll. **a** Main effect plots, **b** two-way factorial interaction

which was found for the power consumption model, while for the specific energy consumption model, R^2 was 98.54%, R^2 (adj.) was 98.41% and R^2 (Pred.) was 98.24%, and for the surface roughness model, R^2 was 97.84%, R^2 (adj.) was 97.65% and R^2 (Pred.) was 97.41%, it reveals the goodness of fit of these models. The second-order regression equations developed by RSM for power consumption, specific energy consumption, and surface roughness by using the CBN tool insert and ceramic tool insert are shown in Table 5. RSM model for the power consumption is shown in Table 6, which revealed that cutting speed, feed, depth of cut, and tool insert all were significant factors with a p value < 0.05, which indicates that these parameters have a statistically significant effect on the power consumption. F-value in these models gives the contribution amount of these parameters to the responses. For the power consumption model, cutting speed with the F-value of 694.4 was found to be the most contributing factor (48% contribution), and it was followed by tool insert type (16.27% contribution), feed (15.27% contribution), and depth of cut (3.33% contribution). Table 7 shows the RSM model for specific energy consumption. It revealed that feed was the highest contributing factor with 54.51% contribution for specific energy consumption, and it was followed by the depth of cut with 34% contribution. The contribution of cutting speed for specific energy consumption was only 0.08%. Table 8 shows the RSM model for the

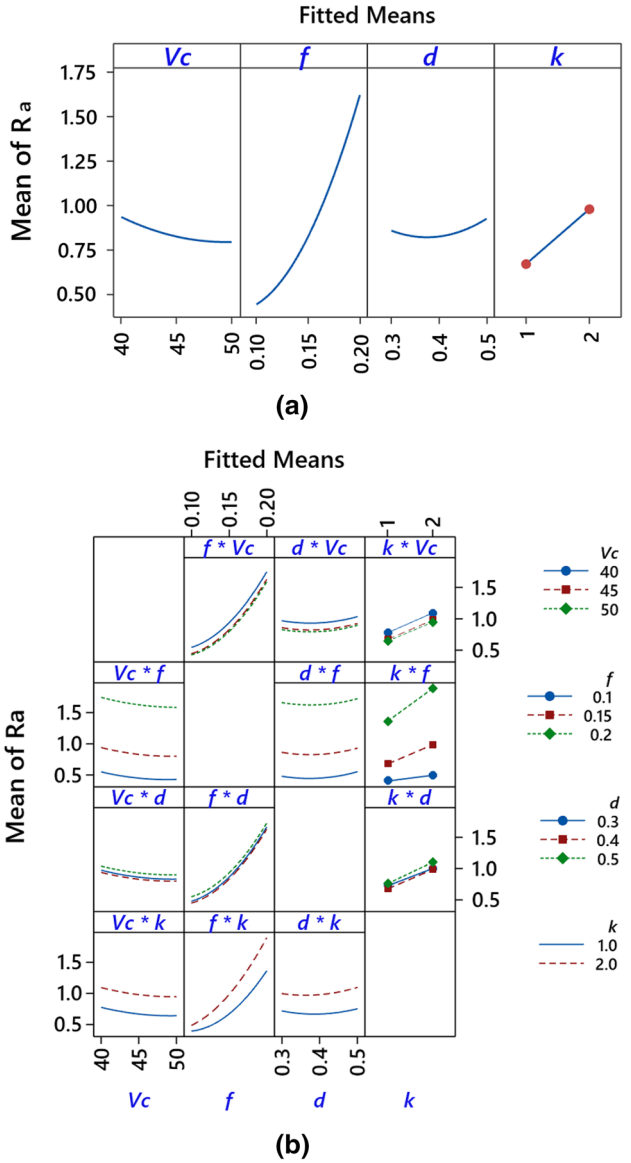

Fig. 7 Factorial plots for surface roughness of the machined surface of the hardened alloy steel roll. **a** Main effect plots, **b** two-way factorial interaction

surface roughness generated on the machined surface of the roll, due to the CNC turning operation. It shows that the feed with an F-value of 5566.3 was the highest contributing factor. The contribution of feed was 81.35%, and it was followed by tool insert type with a 7% contribution. However, the contribution of cutting speed and depth of cut was only 1.15% and 0.26%, respectively.

The main effect plots and the two-way factorial interaction plots for power consumption are shown in Fig. 5a and b, respectively. The main effect plot in Fig. 5a revealed that the minimum power consumption was at the cutting speed of 40 m/min, feed of 0.1 mm/rev, and depth of cut of 0.3 mm with CBN tool insert. Figure 5b shows that the two-way factor's interactions of cutting speed with the feed, the interaction of cutting speed with the depth of cut, and the interaction of feed with the depth of cut were significant.

The main effect plots and the two-way factorial interaction plots for specific energy consumption are shown in Fig. 6a and b, respectively. Figure 6a shows that the mean specific energy consumption was minimum at the feed of 0.20 mm/rev, and the depth of cut of 0.5 mm with the CBN tool insert. The flat line for the cutting speed in Fig. 6a stated that cutting speed was not the main contributing factor to minimize the specific energy consumption. Figure 6b shows that the two-way factor's interactions of the cutting speed with the feed, the interaction of the cutting speed with the cutting tool insert type, the interaction of feed with the depth of cut, the interaction of feed with the cutting tool insert type, and the interaction of depth of cut with the cutting tool insert type, all these interactions were found significant.

The main effect plots and the two-way factorial interaction plots for surface roughness are shown in Fig. 7a and b, respectively. The main effect plots in Fig. 7a revealed that the minimum surface roughness was at the cutting speed of 50 m/min, feed of 0.1 mm/rev, and depth of cut of 0.4 mm with CBN tool insert. Figure 7b shows that the two-way factor's interactions of feed with the cutting tool insert was significant, while the curves all other interaction were found parallel to each other and were insignificant.

3.2 Analysis using Response Contour Plots

A response contour plot, predicated by the quadratic model, was developed to study the effect of input parameters on power consumption, specific energy consumption, and surface roughness as shown in Figs. 8, 9, and 10, respectively. Figure 8 shows the contour plots for the power consumption at three different levels of cutting speed with CBN and ceramic tool inserts. It showed that the contour region for minimum power consumption ($P < 2.7$ kW) was at a cutting speed of 40 m/min with CBN insert, as shown in Fig. 8a. The curved lines of contours shown in surface plots were the indication that both feed and depth of cut have a significant effect on power consumption. The comparison of contours at three different levels of cutting speed with the CBN inserts is shown in Fig. 8a, c, and e. It revealed that the power consumption was increased with the increase in cutting speed. The same results of cutting speed on power consumption were also found with the ceramic tool insert by comparing contour plots, shown in Fig. 8b with d and f. The effect of tool insert material (CBN and Ceramic) on the power consumption was compared at three levels of cutting speed because it was the most contributing factor (48.06%) in the power consumption model. The contour plots at cutting speeds of 40 m/min, 45 m/min, and 50 m/min are illustrated

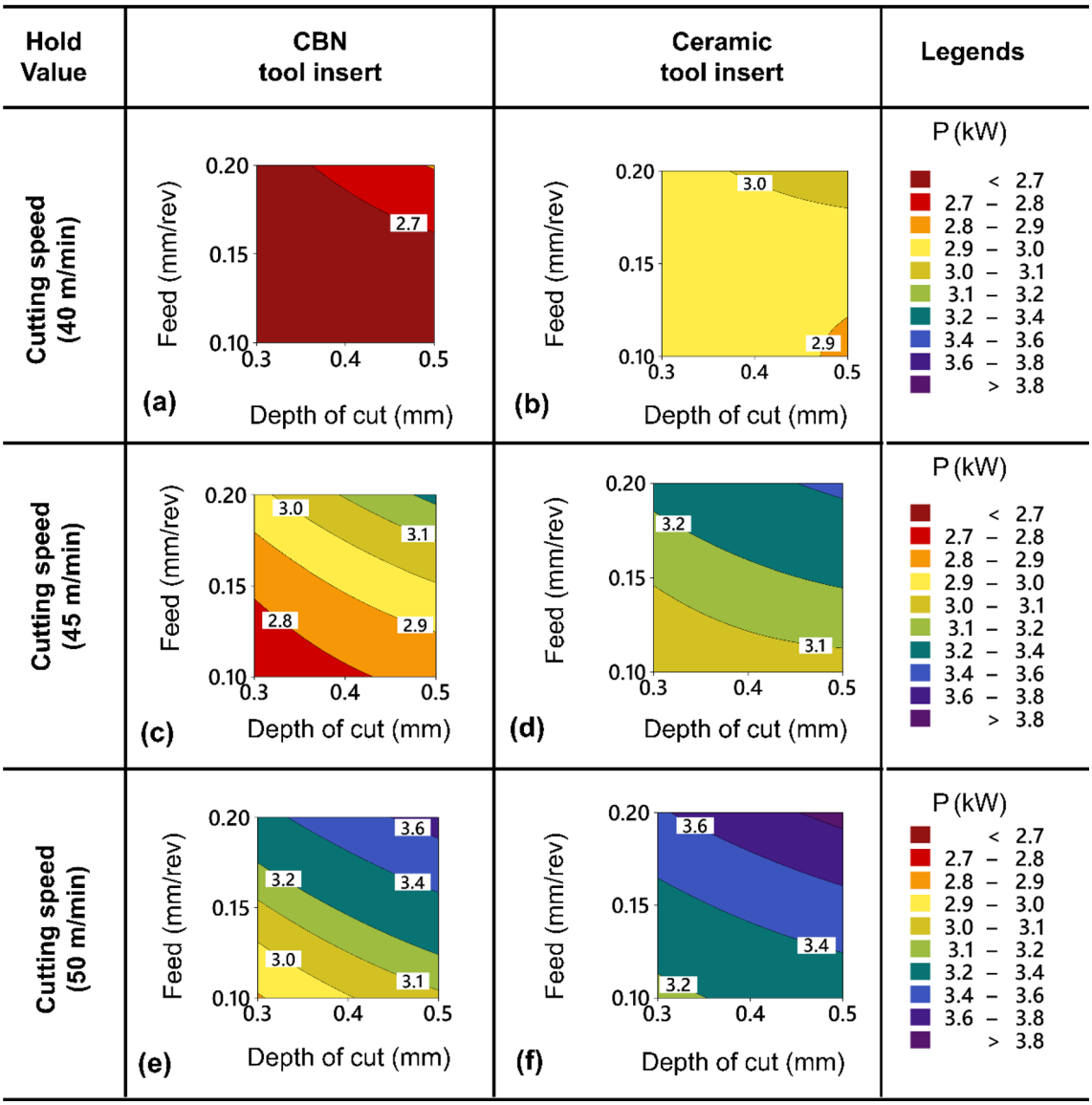

Fig. 8 Contour plots for power consumption in the machining stage of the hardened alloy steel roll by using CBN and ceramic cutting tool inserts at three cutting speed levels

by comparing Fig. 8a with b, comparing Fig. 8c with d and by comparing Fig. 8e with f, respectively. This comparison revealed that the power consumed by the CBN tool insert was lower than the specific energy consumed by the ceramic tool insert at all three corresponding levels of cutting speed.

The contour plots illustration for specific energy consumption is shown in Fig. 9. It showed that the minimum specific energy consumption contour region ($E_s < 0.63$ kJ/mm^3) was at the feed of 0.2 mm/rev with the CBN cutting tool insert, as shown in Fig. 9e. The vertical lines of contours in contour plots were the indication that the cutting speed is not significantly contributing to specific energy consumption and its contribution in the specific energy consumption model is only 0.08%. The comparison of contours at three different levels of feed with the CBN inserts is shown in Fig. 9a, c, and e. It revealed that the specific energy consumption was decreased with the increase in feed level. The same result of feed on the specific energy consumption was observed with the ceramic tool insert by comparing contour plots, as shown in Fig. 9b with d and f. The effect of tool insert material (CBN and ceramic) on specific energy consumption was compared at three levels of feed because it was the most contributing factor (54.51%) in the specific energy consumption model. Contour plots at feed level of 0.10 m/rev, 0.15 mm/rev and 0.20 mm/rev were illustrated by comparing Fig. 9a with b, comparing Fig. 9c with d and by comparing Fig. 9e with

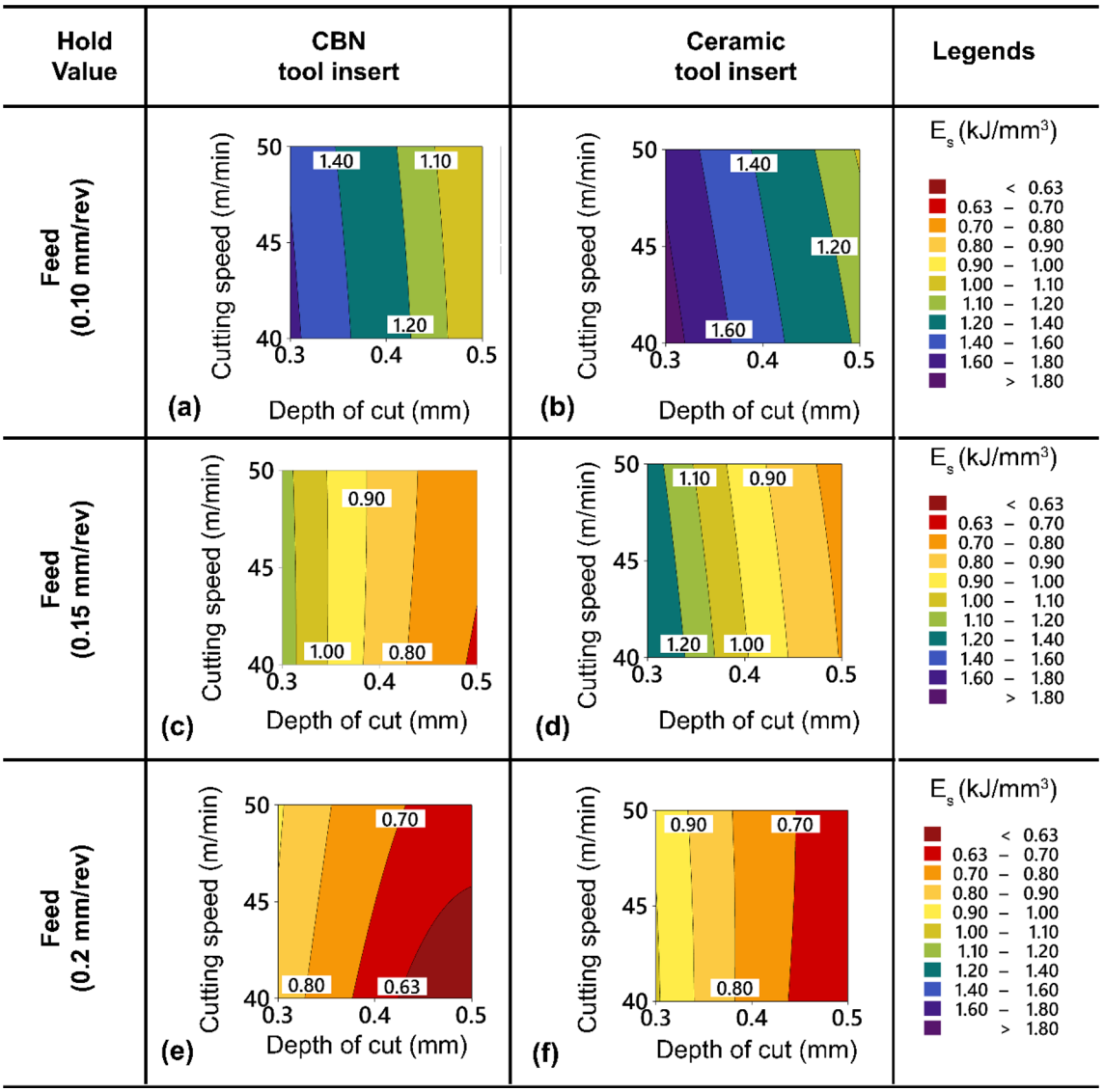

Fig. 9 Contour plots for specific energy consumption in the machining stage of the hardened alloy steel roll by using CBN and ceramic cutting tool inserts at three feed levels

f, respectively. This comparison revealed that the specific energy consumed by the CBN tool insert was lower than the specific energy consumed by the ceramic tool insert at all three corresponding levels of feed.

Figure 10 shows the contour plots for the surface roughness at three different levels of feed with CBN and ceramic tool inserts. The effect of cutting tool insert type (CBN and Ceramic) on the surface roughness was compared at three levels of feed since the feed was found to be the highest contributing factor (81.35%) in the surface roughness model. This comparison at three different feeds showed that the surface roughness was decreased with a decrease in feed for both the CBN and the ceramic cutting tool inserts. The comparison of surface roughness by using the CBN and the ceramic cutting tool inserts at feed 0.1 m/min are shown in Fig. 10a and b, respectively, and it shows that surface roughness values obtained by using the CBN cutting tool insert were lower than the surface roughness obtained by using the ceramic cutting tool insert. The contour region for minimum surface roughness contour region ($R_a < 0.4$ µm) was at the feed of 0.1 mm/rev with CBN insert, and it is shown in Fig. 10a.

3.3 Optimization Using Desirability Function

The desirability function is an attractive optimization technique used for various industrial problems. Initially, each

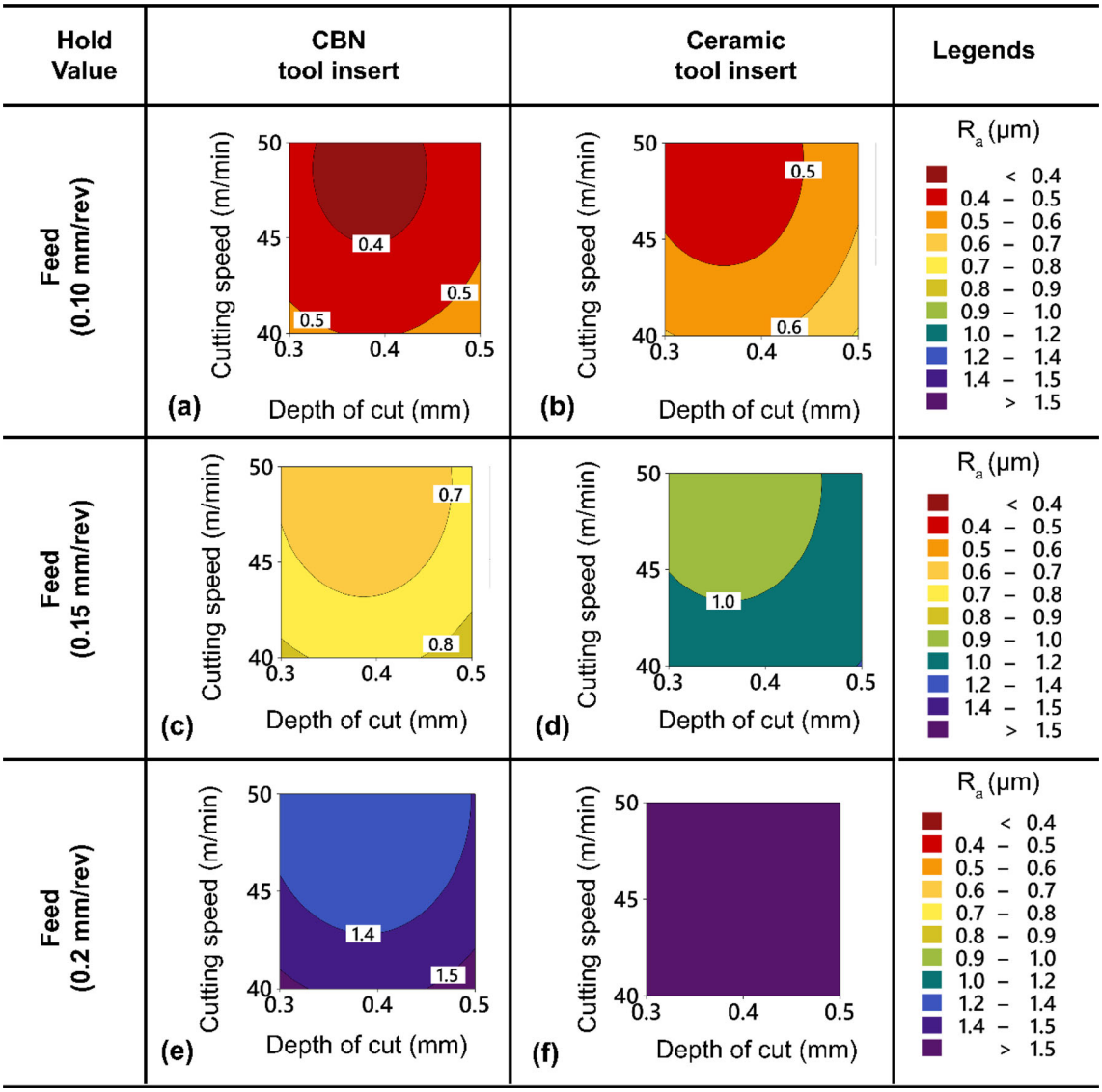

Fig. 10 Contour plots for surface roughness produced at the machined surface of the roll by using CBN and ceramic cutting tool inserts at three feed levels

response y_i is converted into an individual desirability function Δ_i that varies over the range of 0 to 1. If the goal is minimization and response y_i is less than the target value T, Δ_i is taken as 1, it represents the ideal case. If response y_i is higher than the target value T, Δ_i is taken zero, it represents an unacceptable configuration for the selected response. If response y_i lies between target and upper value, Δ_i lies between 1 and 0. The individual desirability function given by Eq. (4) is used to search the optimal solution for minimization [26].

$$\Delta_i = \begin{cases} 1 & y_i < T \\ \left(\frac{U-y_i}{U-T}\right)^r & T \le y_i \le U \\ 0 & y_i > U \end{cases} \tag{4}$$

where Δ_i is the individual desirability defined for the ith targeted output, U is the upper limit value, T is the target value, and r is the desirability function index.

The composite desirability is the geometric mean of all the individual values of desirability and is given by Eq. (5):

$$D = (\Delta_1.\Delta_2.\Delta_3 \ldots \Delta_m)^{\frac{1}{m}} \tag{5}$$

where m is the number of responses.

Table 9 represents the goal and target range used in optimization. The optimal solution was found at a composite desirability value of 0.9345, having a response fit value was 2.709 kW for power consumption and 0.7855 kJ/mm^3 for specific energy consumption, and 0.6796 μm for surface

Table 9 Goal and target used in optimization

Constraints	Goal	Target	Upper limit	Weight	Importance
Power consumption (kW)	Minimization	2.71	4.09	1	1
Specific energy consumption (kJ/mm^3)	Minimization	0.68	2.211	1	1
Surface roughness (μm)	Minimization	0.49	1.95333	1	1

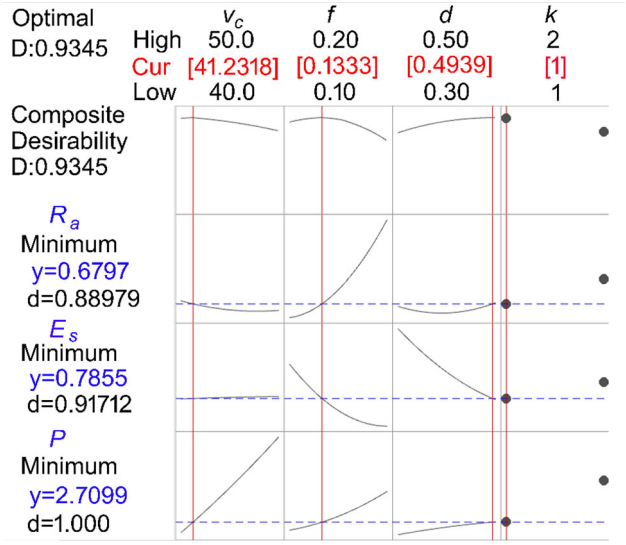

Fig. 11 Optimum solution obtained by using the desirability function

roughness. The corresponding values of optimum parameters were cutting speed of 41.2318 m/min, feed of 0.1333 mm/rev, and depth of cut of 0.4939 mm with CBN cutting tool insert as shown in Fig. 11. The experimental validity at the optimal parameters in Table 10 shows that a 3.16% error in power consumption, 4.5% error in specific energy consumption, and 4.28% error in surface roughness were observed between the predicted value and the experimental value performed at optimal machining parameters.

4 Conclusion

This experimental study was carried out to perform a CNC turning operation on a large-sized, hardened alloy steel roll, at a low cutting speed, under wet machining conditions. The aim was to determine out the optimized machining parameters that consumed minimum power, and minimum specific energy to produce a machined surface of the roll with minimum surface roughness. The results obtained in the experimental study, at three different levels of cutting speeds, feeds, and depth of cuts with the use of two different types of cutting tool inserts, CBN and ceramic are as follows:

- RSM full quadratic models reported that cutting speed was the highest contributing factor for power consumption and feed was the highest contributing factor for both the specific energy consumption and the surface roughness.
- The cutting tool insert type was found statistically significant factor for power consumption, specific energy consumption, and surface roughness
- The comparison of contour plots between the CBN and the Ceramic cutting tool inserts reported that the CBN cutting tool inserts were more effective than the Ceramic cutting tool inserts, at low cutting speeds and under wet machining conditions. The lowest contour line for the minimum power consumption ($P < 2.7$ kW) was found at a cutting speed of 40 m/min with the CBN cutting tool insert, the lowest contour line for the minimum specific energy consumption ($E_s < 0.63$ kJ/mm^3) was found at the feed of 0.2 mm/rev with the CBN cutting tool insert, and the lowest contour line for the minimum surface roughness (Ra < 0.4 μm) was found at the feed of 0.1 mm/rev with the CBN cutting tool insert.

Table 10 Validation of model showing predicted and experimental values at optimal machining parameters

Machining characteristics	Optimal parameters (V_c, f, d, k)	Predicted value	Experimental value	Error (%)
Power consumption (kW)	(41.2318, 0.1333, 0.4938, CBN)	2.70	2.79	3.16
Specific energy consumption (kJ/mm^3)	(41.2318, 0.1333, 0.4938, CBN)	0.79	0.83	4.5
Surface roughness (μm)	(41.2318, 0.1333, 0.4938, CBN)	0.672	0.701	4.28

- Desirability analysis found that the cutting speed of 41.23 m/min, feed of 0.133 mm/rev, depth of cut of 0.49 mm with the CBN cutting tool insert were the optimized machining parameters, and the predicted power consumption was 2.709 kW, predicted specific energy consumption was 0.785 kJ/mm^3, and predicted surface roughness of machined surface was 0.679 μm.

Collectively, this may be summarized that the CBN tool inserts were more effective than the ceramic tool inserts, for CNC turning of large-sized hardened alloy steel at low cutting speed under wet machining conditions.

Acknowledgements The authors are grateful for the support of Amreli Steels Limited, Pakistan (Dhabeji Plant), for providing the material (alloy steel roll) and for providing the workshop facility. The authors are also thankful to the Electronics Department of NED University of Engineering & Technology, Pakistan, for providing the Fluke device for recording power consumption data.

Author contributions KN developed and formulated the methodology, performed the experimental work, analyzed the results, and drafted the manuscript. MAS supervised the project, helped in developing experimental plans and samples, reviewed the drafted paper, and addressed revision. SAI co-supervised the project, reviewed the drafted paper, and assisted in experimental plans.

Data availability All the data used in this paper can be obtained from the corresponding author upon request.

Declarations

Conflict of interest The authors declare that they do not have any conflict of interest.

References

1. Shin, S.-J.; Woo, J.; Rachuri, S.; Meilanitasari, P.: Standard data-based predictive modeling for power consumption in turning machining. Sustainability. **10**(3), 598 (2018). https://doi.org/10.3390/su10030598
2. Kara, S.; Li, W.: Unit process energy consumption models for material removal processes. CIRP Ann. Manuf. Technol. **60**(1), 37–40 (2011). https://doi.org/10.1016/j.cirp.2011.03.018
3. Padhan, S.; Dash, L.; Behera, S.K.; Das, S.R.: Modeling and optimization of power consumption for economic analysis, energy-saving carbon footprint analysis, and sustainability assessment in finish hard turning under graphene nanoparticle–assisted minimum quantity lubrication. Process Integr. Optim. Sustain. **4**(4), 445–463 (2020). https://doi.org/10.1007/s41660-020-00132-9
4. Benlahmidi, S.; Aouici, H.; Boutaghane, F.; Khellaf, A.; Fnides, B.; Yallese, M.: Design optimization of cutting parameters when turning hardened AISI H11 steel (50 HRC) with CBN7020 tools. Int. J. Adv. Manuf. Technol. **89**(1–4), 803–820 (2017). https://doi.org/10.1007/s00170-016-9121-3
5. Chudy, R.; Grzesik, W.: Comparison of power and energy consumption for hard turning and burnishing operations of 41Cr4 steel. J. Mach. Eng. **15**(4), 113–120 (2015)
6. Żak, K.: Cutting mechanics and surface finish for turning with differently shaped CBN tools. Arch Mech. Eng. (2017). https://doi.org/10.1515/meceng-2017-0021
7. Bilga, P.S.; Singh, S.; Kumar, R.: Optimization of energy consumption response parameters for turning operation using Taguchi method. J. Clean. Prod. **137**, 1406–1417 (2016). https://doi.org/10.1016/j.jclepro.2016.07.220
8. Zerti, O.; Yallese, M.A.; Khettabi, R.; Chaoui, K.; Mabrouki, T.: Design optimization for minimum technological parameters when dry turning of AISI D3 steel using Taguchi method. Int. J. Adv. Manuf. Technol. **89**(5–8), 1915–1934 (2017). https://doi.org/10.1007/s00170-016-9162-7
9. Grzesik, W.; Żak, K.; Chudy, R.: Influence of tool nose radius on the cutting performance and surface finish during hard turning with CBN cutting tools. J. Mach. Eng. **17**(2), 56–64 (2017)
10. Park, H.-S.; Nguyen, T.-T.: Multi-objective optimization of turning process for hardened material based on hybrid approach. J. Adv. Mech. Des. Syst. Manuf. **10**(8), JAMDSM0101 (2016). https://doi.org/10.1299/jamdsm.2016jamdsm0101
11. Nguyen, T.-T.; Duong, Q.-D.; Mia, M.: Sustainability-based optimization of the rotary turning of the hardened steel. Metals. **10**(7), 939 (2020). https://doi.org/10.3390/met10070939
12. Nguyen, T.-T.: An energy-efficient optimization of the hard turning using rotary tool. Neural Comput. Appl. **33**(7), 2621–2644 (2021). https://doi.org/10.1007/s00521-020-05149-2
13. Zębala, W.; Siwiec, J.: Hard turning of cold work tool steel with CBN tools. Adv. Manuf. Sci. Technol. **36**(4), 19–32 (2012)
14. Bouacha, K.; Yallese, M.A.; Mabrouki, T.; Rigal, J.-F.: Statistical analysis of surface roughness and cutting forces using response surface methodology in hard turning of AISI 52100 bearing steel with CBN tool. Int. J. Refract. Hard Met. **28**(3), 349–361 (2010). https://doi.org/10.1016/j.ijrmhm.2009.11.011
15. Das, S.R.; Kumar, A.; Dhupal, D.: Experimental investigation on cutting force and surface roughness in machining of hardened AISI 52100 steel using cBN tool. Int. J. Mach. Mach. Mater. **18**(5–6), 501–521 (2016). https://doi.org/10.1504/IJMMM.2016.078997
16. Bensouilah, H.; Aouici, H.; Meddour, I.; Yallese, M.A.; Mabrouki, T.; Girardin, F.: Performance of coated and uncoated mixed ceramic tools in hard turning process. Measurement **82**, 1–18 (2016). https://doi.org/10.1016/j.measurement.2015.11.042
17. Suresh, R.; Basavarajappa, S.: Effect of process parameters on tool wear and surface roughness during turning of hardened steel with coated ceramic tool. Procedia Mater. Sci. **5**, 1450–1459 (2014). https://doi.org/10.1016/j.mspro.2014.07.464
18. Davoudinejad, A.; Noordin, M.: Effect of cutting edge preparation on tool performance in hard-turning of DF-3 tool steel with ceramic tools. J. Mech. Sci. Technol. **28**(11), 4727–4736 (2014). https://doi.org/10.1007/s12206-014-1039-9
19. Benga, G.C.; Abrao, A.M.: Turning of hardened 100Cr6 bearing steel with ceramic and PCBN cutting tools. J. Mater. Process. Technol. **143**, 237–241 (2003). https://doi.org/10.1016/S0924-0136(03)00346-7
20. Aouici, H.; Khellaf, A.; Smaiah, S.; Elbah, M.; Fnides, B.; Yallese, M.: Comparative assessment of coated and uncoated ceramic tools on cutting force components and tool wear in hard turning of AISI H11 steel using Taguchi plan and RMS. Sādhanā. **42**(12), 2157–2170 (2017). https://doi.org/10.1007/s12046-017-0746-1
21. Anthony, X.: Analysis of cutting force and chip morphology during hard turning of AISI D2 steel. J. Eng. Sci. Technol. **10**(3), 282–290 (2015)
22. Cui, X.; Guo, J.: Identification of the optimum cutting parameters in intermittent hard turning with specific cutting energy, damage equivalent stress, and surface roughness considered. Int. J. Adv. Manuf. Technol. **96**(9–12), 4281–4293 (2018). https://doi.org/10.1007/s00170-018-1885-1

23. Younas, M.; Jaffery, S.H.I.; Khan, M.; Ahmad, R.; Ali, L.; Khan, Z.; Khan, A.: Tool Wear progression and its effect on energy consumption in turning of titanium alloy (Ti–6Al–4V). Mech. Sci. **10**(2), 373–382 (2019)
24. Hussain, S.A.; Pandurangadu, V.; Kumar, K.P.: Cutting power prediction model for turning of GFRP composites using response surface methodology. Int. J. Eng. Sci. Technol. **3**(6), 161–171 (2011)
25. Abhang, L.; Hameedullah, M.: Power prediction model for turning EN-31 steel using response surface methodology. J. Eng. Sci. Technol. Rev. **3**(1), 116–122 (2010). https://doi.org/10.25103/jestr.031.20
26. Montgomery, D.: Design and Analysis of Experiments. John Wiley & Sons Inc., Singapore (2013)